Transactions on Additive Manufacturing Meets Medicine
Trans. AMMM, 2024, Vol. 6, No 1, Article ID 1793, 6 Pages

Infinite Science Publishing

Original Research Article

Water-soluble filament in multifilament approach for ultrasound phantom fabrication

C. M. Huber[1,3*], W. Lahmadi[3], A. Alballa[3], C. Heim[4], S. J. Rupitsch[4], H. Ermert[2], I. Ullmann[3], and S. Lyer[3]

[1] *Department of Otorhinolaryngology, Head and Neck Surgery, Section of Experimental Oncology and Nanomedicine (SEON), Professorship for AI-Controlled Nanomaterials (KINAM), Universitätsklinikum Erlangen, Germany*
[2] *Department of Otorhinolaryngology, Head and Neck Surgery, Section of Experimental Oncology and Nanomedicine (SEON), Else Kröner-Fresenius-Stiftung-Professorship, Universitätsklinikum Erlangen, Germany*
[3] *Institute of Microwaves and Photonics (LHFT), Friedrich-Alexander-Universität Erlangen-Nürnberg, Germany*
[4] *Department of Microsystems Engineering (IMTEK), Laboratory for Electrical Instrumentation and Embedded Systems, University of Freiburg, Freiburg, Germany*
[*] *Corresponding author, email: Christian.Ch.Huber@fau.de*

Abstract: Ultrasound phantoms are used in research, equipment testing, calibration, and even in the field of medical training. Despite their importance, commercial ultrasound phantoms are often expensive and may not meet user requirements. While simple phantom construction methods exist which use readily available materials, they often lack versatility in both their exterior and interior designs. By using tissue-mimicking materials such as gelatin, agarose, or polyvinyl alcohol mixed with water, simple yet effective ultrasound phantoms can be created through a heating and hardening process. While designing the outer structure of these phantoms can be achieved through the creation of various molds, crafting complex inner structures poses a more difficult task. Additive manufacturing, specifically fused deposition printing with standard 3D printers, presents a promising solution to this challenge. This involves using soluble materials that can be removed after the phantom hardens. This study aims to simplify the phantom fabrication process and evaluate non-toxic, water-soluble filaments. Using polyvinyl alcohol (PVA) filament in combination with high-impact polystyrene (HIPS) is a promising approach. A tumor sacrificial mold is printed with PVA, while the vascular sacrificial structure is printed with HIPS. First, the tumor-mimicking material is filled into the PVA mold, which is then dissolved with water. Next, the tumor model with the HIPS flow structure is submerged in the tissue-mimicking material. Subsequently, the flow structure is dissolved with D-(+) limonene, leaving wall-less flow channels in the ultrasound phantom. The successful fabrication of the phantom is demonstrated through optical images and 3D ultrasound measurements.

I. Introduction

Ultrasound phantoms play a vital role in research and development, the training of medical personnel before transitioning to animal and human subjects, and the maintenance and calibration of medical equipment. Conducting experiments directly on animals or humans raises ethical and moral considerations and needs careful planning and extensive bureaucratic effort. Hence, it is important for ultrasound phantoms to closely replicate real-world environments. The ultrasound parameters of these phantoms primarily hinge on the chosen tissue-mimicking material (TMMs), alongside the preparation process. Agarose, gelatin, and polyvinyl alcohol (PVA) are commonly used TMMs. To fabricate standard ultrasound phantoms, TMM powder is mixed with a scattering agent (graphite [1], silica gel [2] or other microparticles [3]) and ultrapure water. This mixture is heated under constant stirring and then hardened either in a refrigerator or freezer.

The effectiveness of ultrasound phantoms depends not only on their ultrasound parameters, but also on their outer and inner structure. The phantoms must be designed to simulate various biological contexts, such as cardiovascular flow [4] and cancerous tissue [5]. Given that cardiovascular diseases stand as the leading cause of global mortality [6],

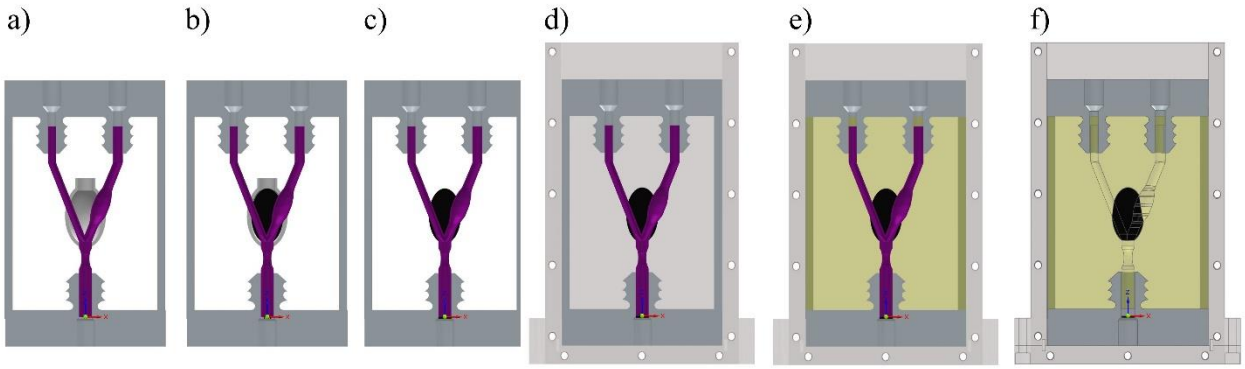

Figure 1: Illustration of the fabrication process (gray: supporting scaffold in ABS; violet: sacrificial flow scaffold in HIPS; and white: sacrificial tumor scaffold in PVA): a) the sacrificial tumor and flow scaffold is printed and placed within the supporting scaffold; b) tumor mimicking material is filled inside the sacrificial tumor mold; c) the sacrificial tumor mold is dissolved with water at 30 °C; d) the scaffold is now placed inside an outer mold; e) tissue mimicking material is filled inside the outer mold, fully submerging the sacrificial scaffold; and f) the sacrificial flow structure is dissolved with HIPS.

followed closely by the various forms of cancer [7], the replication of such scenarios within ultrasound phantoms holds immense importance.

Additive manufacturing, which has already been employed in the medical field for producing equipment against COVID-19 [8, 9], medical aids and devices [10], and scaffolds [11], can enable the replication of complex scenarios in ultrasound phantoms. To enable the replication of these scenarios within ultrasound phantoms, it is essential for both the surface and the underlying structures to be adaptable to the needs of the experiments. This adaptability can be achieved through additive manufacturing.

Fused deposition modeling (FDM) 3D printing was utilized to craft soluble structures that can be used as model for cardiovascular flow [12, 13, 14]. These soluble structures are inserted into the still fluid ultrasound phantom mixture, and after hardening, the structure is flushed out. The authors of [12] utilized PVA to create such soluble structures and corresponding flow channels. The principal challenge associated with PVA filament is its rapid dissolution associated with and deformation in aqueous solutions, which can impede its use in water-based ultrasound phantoms. To mitigate this problem, the authors in [12] used paraffin wax coating on the contact side with the ultrasound phantom. PVA needs water as a solvent, which is easy to handle and non-toxic. The authors of [13, 14] used polylactic acid (PLA) filament for the same process. Here, the solvent is chloroform. PLA does not dissolve or deform when immersed in water-based ultrasound phantoms, but the solvent is potentially harmful for humans.

A similar process can also be done using stereolithography (SLA) 3D printer and water-soluble resin [15]. It is important to note that complete 3D-printing systems are the topic of research, which can print arbitrary ultrasound phantoms, but these are still limited to a small number of research institutes and are expensive to construct or acquire [16, 17, 18, 19, 20].

In our previous research [21], we demonstrated the application of high impact polystyrene (HIPS) in creating complex flow channels within phantoms. Building upon this, in our latest study [22] we developed a more sophisticated practical setting, featuring the fabrication of a carotid bifurcation tumor. In this setting, the capability of using multiple soluble filaments (HIPS and VXL70) to generate not just vascular flow, but also the integration of a tumor structure was illustrated. VXL70 needs sodium hydroxide as solvent. This solvent is potentially harmful for humans and can also affect the ultrasound phantoms, potentially even dissolving it, which means, that care must be taken when creating ultrasound phantoms with VXL70.

This contribution evaluates PVA filament as a potential alternative to VXL70. PVA filament was used as a sacrificial tumor structure in combination with HIPS as a sacrificial flow structure. PVA uses water as a solvent, which does not negatively interact with the water-based ultrasound phantoms and is non-toxic. Although PVA has previously been used for fabricating flow structures [12], it has not been employed in a multifilament approach, highlighting its significant potential in this context. However, because PVA is affected by the solvent used for HIPS, the PVA sacrificial tumor structure must be dissolved before the HIPS sacrificial flow structure.

II. Material and methods

Here, the steps of the phantoms fabrication and evaluation will be described. See Figure 1 for an overview of the fabrication steps and Figure 2 for the geometric details.

II.1 Sacrificial scaffolds

Until now, PLA [13, 14], HIPS [21] and PVA [12] were used in the fabrication of normal vascular ultrasound phantoms. VXL70 (with HIPS as vascular scaffold) was utilized to include a tumor structure [22]. In this

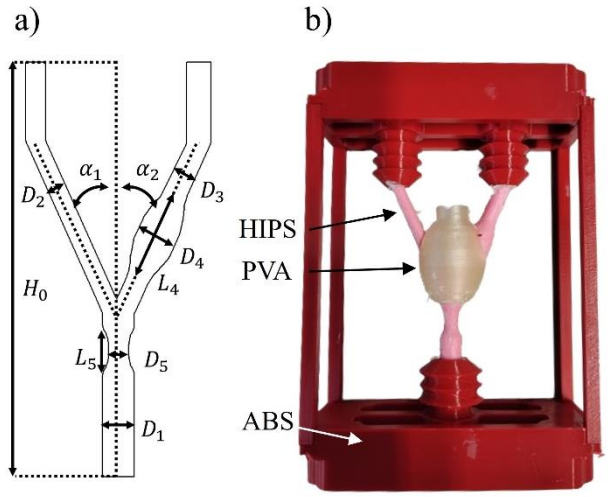

Figure 2: a) Illustration of carotid bifurcation with aneurysm (widening of flow channel) and plaque (narrowing of flow channel), adapted from [23] ($H_0 = 100$ mm, $\alpha_1 = \alpha_2 = 15°$, $D_1 = 8$ mm, $D_2 = 4.6$ mm, $D_3 = 5.8$ mm, $D_4 = 10$ mm, $L_4 = 20$ mm, $D_5 = 5$ mm, $L_5 = 12$ mm). The tumor is an ellipsoid with a diameter of 20 mm and a length of 40 mm. b) shows the printed structures in the supporting scaffold, with polyvinyl alcohol (PVA, white) filament, high impact polystyrene (HIPS, pink) and acrylonitrile butadiene styrene (ABS, red).

contribution, a combination of PVA and HIPS are used for the fabrication of a vascular tumor ultrasound phantom. These scaffolds were printed with the Flashforge Creator Pro 2, which is an independent double extrusion system (IDEX) printer. The IDEX system allows for the seamless printing of two materials, without any waste, as it features two extruders.

The sacrificial tumor and vascular scaffold will now be described:

- Sacrificial tumor scaffold
  The tumor model was a simplified representation of a Type III carotid body tumor, as classified by the Shamblin system [24]. The tumor, which typically envelops both carotid arteries, was depicted as an ellipsoid with a diameter of 20 mm and a length of 40 mm. To mimic the tumor material, a mixture of 3 wt% agarose and 1 wt% silica gel was used. The structure itself was printed using PVA filament (Xioneer Systems GmbH, soluble support material), with water serving as the solvent.

- Sacrificial vascular scaffold
  The vascular scaffold was designed based on a carotid bifurcation with malformations, adapted from [23]. A carotid bifurcation consists of the internal carotid artery (ICA) and the external carotid artery (ECA). In this model, the ICA is the narrower artery (left flow channel in Figure 2), while the ECA is the larger one (right channel in Figure 2). The malformations include a plaque (narrowing of the flow channel) below the tumor structure and an aneurysm (widening of the flow channel) on the ECA. This structure is printed using HIPS filament (Nunus filament, Keycoon GmbH), with D-(+)-limonene (Carl Roth GmbH & Co. KG) used as the solvent.

PVA was chosen for the tumor scaffold and HIPS for the vascular scaffold, with the dissolution process starting with the tumor scaffold followed by the vascular scaffold. Since PVA is affected by the solvent D-(+) limonene, it had to be dissolved before the HIPS scaffold.

II.2 Fabrication steps

To fabricate vascular ultrasound phantoms with a tumor inclusion, the first step in the presented attempt was to print the soluble scaffolds using two filaments (Figure 1a), with two distinctive solvents, which do not affect the respective other filament, when dissolved in the correct order. PVA-filament for the sacrificial tumor scaffold and HIPS for the sacrificial vascular scaffold are utilized. This order was chosen, as the tumor scaffold was dissolved before the vascular structure. Water (solvent of PVA) does not affect HIPS, but D-(+)-limonene (solvent of HIPS) does affect PVA.

In the second step (Figure 1b), the tumor mimicking material was prepared. Here, agarose with scattering agents is used. The generation of the tumor and tissue mimicking material will be described in more detail in Subsection *II.3 Tumor and Tissue Mimicking Phantoms*. The tumor mimicking mixture was then poured into the sacrificial tumor scaffold and allowed to harden in a refrigerator for 6 hours. After hardening, the sacrificial tumor scaffold was dissolved in water for 24 hours (Figure 1c), where only the tumor mimicking phantom remained. Subsequently, the whole scaffold was placed in the outer mold (Figure 1d). The tissue mimicking material, which was agarose without scattering agent, was prepared, and poured in the outer mold, submerging the whole scaffold (Figure 1e). It was then placed in the refrigerator for 6 hours to allow the mixture to harden. After hardening, tubes and a pump were connected to the scaffold and the solvent for the sacrificial vascular structure (D-(+)-limonene for HIPS) was pumped through it using a peristaltic pump (Pharmacia LKB P-1). The dissolution process took at least 6 hours. After dissolution of the sacrificial vascular structure, the ultrasound phantom was completed (Figure 1f).

II.3 Tumor and tissue mimicking phantoms

To evaluate the fabrication process of the complex ultrasound phantom, the TMMs used for the tumor inclusion and the tissue were slightly different. The tissue mimicking phantom will be described first, as the tumor mimicking phantom is only a slight alteration. Agarose was used as TMMs for these phantoms, as agarose-based

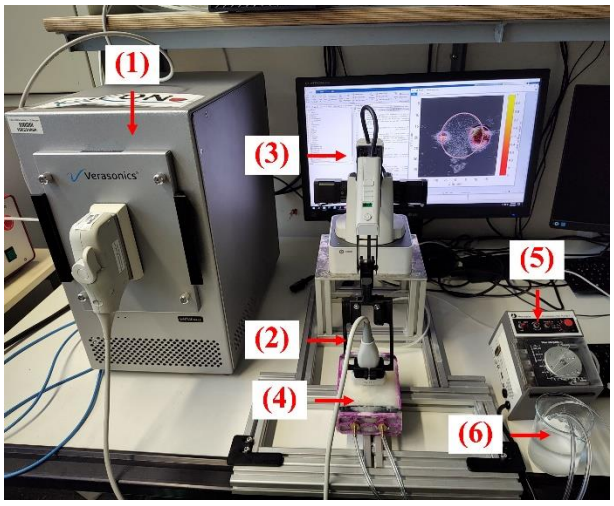

Figure 3: Ultrasound measurement setup showing (1) the Verasonics vantage 64 LE ultrasound system, (2) the ultrasound transducer, (3) the Dobot Magician robotic arm, (4) the ultrasound phantom, (5) the peristaltic pump, and (6) the blood mimicking fluid.

phantoms can be easily modified using difference wt% agarose to mimic different types of tissue or different levels of stiffness [25].

For the tissue mimicking phantom, 99 wt% of ultrapure water was mixed with 1 wt% agarose powder (Agarose Standard; CHEMSOLUTE). The water-agarose mixture was then heated to 90 °C while constantly stirred with a magnetic stirrer (C-MAG HS 7, IKA-Werke GmbH & CO. KG) until the mixture was completely clear. Then, it could be poured into the outer mold. For the tumor mimicking phantom, 3 wt% of agarose and 1 wt% of silica gel (used as scattering agent; ROTH silica gel 60, particle size from 40 µm to 60 µm) was used instead, with all other steps the same. A higher wt% of agarose and added scattering agents were used to track the tumor mimicking phantom using ultrasound B-mode information, as described in the next subsection.

II.3 Ultrasound Measurements

To confirm the successful fabrication of the vascular tumor ultrasound phantom, different ultrasound measurements were taken in a three-dimensional manner. For that, a measurement setup as shown in Figure 3 was used. An ultrasound system (Verasonics Vantage 64 LE) with a linear array (Verasonics L11-5v; center frequency of 7.6 MHz; 128 elements; 0.3 mm pitch; and 77 % relative bandwidth) acquired ultrasound B-mode and ultrasound Doppler information of the ultrasound phantom, where a blood mimicking fluid (BMF) was pumped through the phantoms using a peristaltic pump (Pharmacia LKB P-1). The acquired ultrasound Doppler data was integrated over a period of one second for each position to allow complete imaging of the flow channel, as turbulent flow was present.

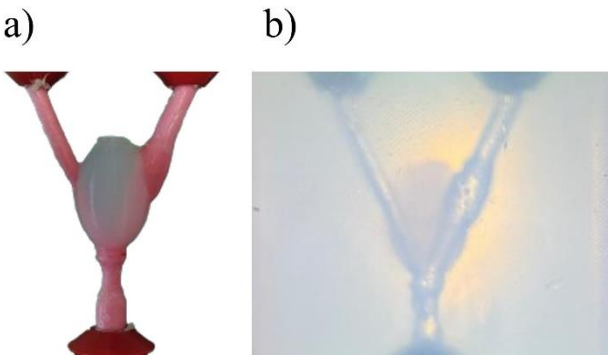

Figure 4: Results of the dissolution process in step c) and f) of Figure 1. In a) the polyvinyl alcohol filament is dissolved, leaving only the tumor mimicking phantom. In b) the complete phantom is shown with the tumor inclusion slightly visible and the wall-less flow channel. Note that background lighting was needed, which leaves a yellow tone in image b).

The BMF was composed of 85 wt% pure water, 3 wt% dextran (ROTH dextran 40), 10 wt% glycerol (ROTH glycerol ROTIPURAN), and 2 wt% silica gel (ROTH silica gel 60, particle size from 40 µm to 60 µm). The ultrasound transducer was placed into a 3D printed holding structure, which was fixed to a robotic arm (Dobot Magician). The ultrasound transducer was oriented orthogonally to the start and end of the flow channels, as shown in Figure 3. The robotic arm displaced the ultrasound transducer in 0.5 mm steps along the ultrasound phantom. The obtained 2D ultrasound slices were aligned along the displacement direction to form a 3D ultrasound volume, providing either Doppler information for flow assessment or B-mode information for tumor evaluation. Due to the higher wt% of agarose and the added scattering agent, the tumor mimicking phantom can be distinguished in the ultrasound B-mode images.

III. Results and discussion

The results of the dissolution processes for either PVA or HIPS filament is shown in Figure 4. In Figure 4a, the sacrificial tumor scaffold is already dissolved, which only leaves the tumor mimicking phantom. The tumor mimicking phantom was now held in place thanks to the sacrificial vascular scaffold. Figure 4a represents the successful step c, which is presented in Figure 1c. The final phantom is depicted in Figure 4b, where a backlight illuminates the phantom for better visibility of the tumor and vascular structures. The tumor mimicking phantom is slightly visible, but the now wall-les flow channels are clearly visible. Figure 4 demonstrates the successful fabrication of a vascular tumor ultrasound phantom using PVA and HIPS as soluble structures. The solvents used for PVA (water) and HIPS (D-(+) limonene) did not dissolve the ultrasound phantom, indicating promising potential for use. However, further evaluation is necessary to determine

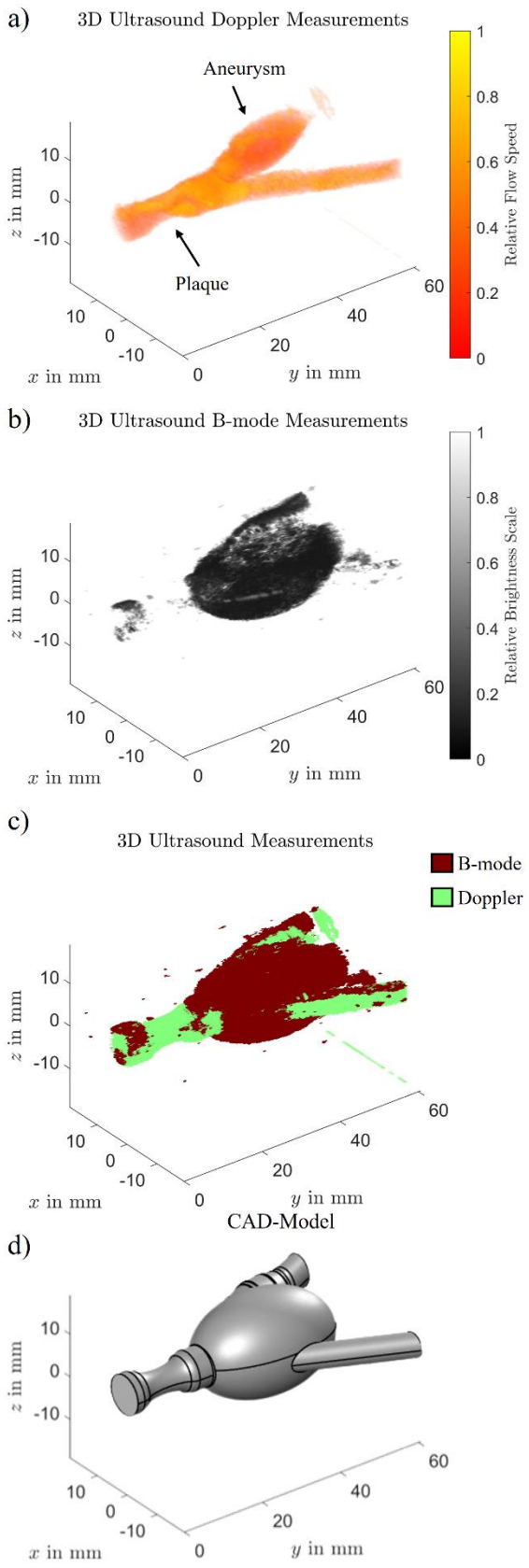

Figure 5: 3D ultrasound measurements of the completed complex ultrasound phantom shown in Figure 4b. a) demonstrates the flow inside the phantom using ultrasound power Doppler imaging; b) shows the tumor inclusion suing B-mode measurements; in c) these measurements are overlaid illustrating the regions of interest; and in d) the CAD-Model is shown as comparison.

if these solvents alter the ultrasound parameters of the phantoms, especially for D-(+) limonene.

In Figure 5, the resulting ultrasound measurements of the ultrasound phantom shown in Figure 4b are presented. In Figure 5a, the 3D ultrasound power Doppler information is shown. Here, the flow channels and the malformations are visible. A narrowing of flow is shown at the beginning (plaque in Figure 5a), while a widening is also present (aneurysm in Figure 5a). In Figure 5b, the 3D ultrasound B-mode image of the tumor inclusion is shown, and the flow channels are slightly visible. In Figure 5c, both 3D Doppler and 3D B-mode are overlaid. Comparing the 3D ultrasound volume to the CAD-Model in Figure 5d, the complete and successful fabrication of the vascular tumor ultrasound phantom is demonstrated again.

IV. Conclusions

In this contribution, an approach for the fabrication of vascular ultrasound phantoms with a tumor inclusion using a novel combination of soluble filaments was demonstrated. In our previous work, the combination of VXL70 and HIPS was used, where VXL70 needed a solvent, sodium hydroxide, which is potentially harmful and can also dissolve the ultrasound phantom material, if not carefully used. In this contribution, a combination of PVA and HIPS was used, with PVA serving as the sacrificial tumor scaffold and HIPS as the sacrificial vascular scaffold. This arrangement enabled the straightforward fabrication of complex ultrasound phantoms. Due to the effect of D-(+) limonene on PVA, PVA had to be dissolved first, followed by HIPS. The successful creation of these phantoms was demonstrated through optical images and ultrasound measurements.

PVA, compared to the previously used VXL70, was more easily dissolved without the use of a potentially harmful solvent. The disposal of the remaining solvent (water with PVA) can be done easily over the sink, while sodium hydroxide with VXL70 needs special disposal. These two advantages show that PVA was a better fit than VXL70 for the fabrication of vascular tumor ultrasound phantoms. If more than two dissolution steps are needed, which necessitates more than two distinct soluble filaments, VXL70 can still find application in the fabrication. Other possible filaments are PLA with chloroform as solvent, ABS with acetone, BVOH with water and VXL90 with sodium hydroxide. All these types of filaments have their advantages and disadvantages, which must be carefully evaluated for the fabrication of complex ultrasound phantoms.

In future work, the solution process of different filaments and their suitability for the fabrication of complex ultrasound phantoms will be evaluated. Additionally, more complex structures will be created and utilized in ultrasonic experiments.

ACKNOWLEDGMENTS

The authors gratefully acknowledge the financial support of the German Research Foundation (DFG) - project number 452821018, and the Julitta und Richard Müller Stiftung.

AUTHOR'S STATEMENT

Conflict of interest: Authors state no conflict of interest. Animal models: No animal experiments were carried out. Informed consent: Informed consent has been obtained from all individuals included in this study. Ethical approval: No material directly derived from animals or humans was used conducting this study.

REFERENCES

[1] E. L. Madsen, J. A. Zagzebski, R. A. Banjavie, & R. E. Jutila, Tissue mimicking materials for ultrasound phantoms, Medical Physics, 5(5), 391-394, 1978.

[2] L. K. Ryan, & F. S. Foster, Tissue equivalent vessel phantoms for intravascular ultrasound, Ultrasound in Medicine & Biology, 23(2), 261-273, 1997.

[3] V. Uhlendorf, Physics of ultrasound contrast imaging: scattering in the linear range, IEEE Transactions on Ultrasonics, Ferroelectrics, and Frequency Control, 41(1), 70-79, 1994.

[4] W. Dabrowski, J. Dunmore-Buyze, H. N. Cardinal, & A. Fenster, A real vessel phantom for flow imaging: 3-D Doppler ultrasound of steady flow, Ultrasound in Medicine & Biology, 27(1), 135-141, 2001.

[5] K. Sugimoto, F. Moriyasu, J. Shiraishi, M. Yamada, & Y. Imai, A phantom study comparing ultrasound-guided liver tumor puncture using new real-time 3D ultrasound and conventional 2D ultrasound, American Journal of Roentgenology, 196(6), W753-W757, 2011.

[6] O. Gaidai, Y. Cao, & S. Loginov, Global cardiovascular diseases death rate prediction. Current Problems in Cardiology, 48(5), 101622, 2023.

[7] J. Ferlay, M. Colombet, I. Soerjomataram, D. M. Parkin, M. Piñeros, A. Znaor, & F. Bray, Cancer statistics for the year 2020: An overview, International Journal of Cancer, 149(4), 778-789, 2021.

[8] M. Schmidt, J. Roitenberg, R. Sims, J. Inziell, F. L. Fenoglietto, & J. Stubbs, Novel design and development process for 3D printed personal protective equipment against COVID-19, Transactions on Additive Manufacturing Meets Medicine, 2(1), 2020.

[9] T. Lück, C. Seifarth, P. Malauschek, O. Schendel, & H. Nopper, Ramping-up 3D-printed corona devices–additive manufacturing opposing injection moulding, Transactions on Additive Manufacturing Meets Medicine, 2(1), 2020.

[10] L. Jonusauskas, T. Baravykas, A. Butkutė, D. Andriukaitis, H. Gricius, T. Tiškūnas, & D. Andrijec, 3D laser microfabrication of medical devices, Transactions on Additive Manufacturing Meets Medicine, 2(1), 2020.

[11] J. Chakka, N. Laird, T. Acri, S. Elangovan, & A. Salem, Polydopamine functionalized 3D printed scaffolds for bone tissue engineering, Transactions on Additive Manufacturing Meets Medicine, 2(1), 2020.

[12] J. Dong, Y. Zhang, & W. N. Lee, Walled vessel-mimicking phantom for ultrasound imaging using 3D printing with a water-soluble filament: design principle, fluid-structure interaction (FSI) simulation, and experimental validation, Physics in Medicine & Biology, 65(8), 085006, 2020.

[13] C. K. Ho, A. J. Chee, B. Y. Yiu, A. C. Tsang, K. W. Chow, & C. H. Alfred, Wall-less flow phantoms with tortuous vascular geometries: Design principles and a patient-specific model fabrication example, IEEE Transactions on Ultrasonics, Ferroelectrics, and Frequency Control, 64(1), 25-38., 2016.

[14] B. Y. Yiu, & C. H. Alfred, Spiral flow phantom for ultrasound flow imaging experimentation, IEEE Transactions on Ultrasonics, Ferroelectrics, and Frequency Control, 64(12), 1840-1848, 2017.

[15] S. Soloukey, B. Generowicz, E. Warnert, G. Springeling, J. Schouten, C. De Zeeuw, C. Dirven, C., A. Vincent, & P. Kruizinga, Patient-Specific Vascular Flow Phantom for MRI-and Doppler Ultrasound Imaging, Ultrasound in Medicine & Biology, 50(6), 860-868, 2024.

[16] M. L. Ommen, M. Schou, C. Beers, J. A. Jensen, N. B. Larsen, & E. V. Thomsen, 3D printed calibration micro-phantoms for super-resolution ultrasound imaging validation, Ultrasonics, 114, 106353, 2021.

[17] R. Zhang, & N. B. Larsen, Stereolithographic hydrogel printing of 3D culture chips with biofunctionalized complex 3D perfusion networks, Lab on a Chip, 17(24), 4273-4282, 2017.

[18] M. L. Ommen, M. Schou, R. Zhang, C. A. V. Hoyos, J. A. Jensen, N. B. Larsen, & E. V. Thomsen, 3D printed flow phantoms with fiducial markers for super-resolution ultrasound imaging. In 2018 IEEE International Ultrasonics Symposium (IUS), pp. 1-9, Oct. 2018.

[19] J. R. Jacquet, F. Ossant, F. Levassort, & J. M. Grégoire, 3-D-Printed phantom fabricated by photopolymer jetting technology for high-frequency ultrasound imaging, IEEE Transactions on Ultrasonics, Ferroelectrics, and Frequency Control, 65(6), 1048-1055, 2018.

[20] S. J. Paulsen, T. M. Mitcham, C. S. Pan, J. Long, B. Grigoryan, D. W. Sazer, C. J. Harlan, K. D. Janson, M. D. Pagel, J. S. Miller, & R. R. Bouchard, Projection-based stereolithography for direct 3D printing of heterogeneous ultrasound phantoms, PLoS One, 16(12), e0260737, 2021.

[21] C. M. Huber, C. Heim, H. Ermert, S. J. Rupitsch, I. Ullmann, & S. Lyer, Wall-less flow phantoms with 3D printed soluble filament for ultrasonic experiments, Current Directions in Biomedical Engineering, 9(1), 97-100, 2023.

[22] C. M. Huber, C. Heim, H. Ermert, S. J. Rupitsch, I. Ullmann, M. Vossiek, & S. Lyer, Ultrasound phantoms of a carotid bifurcation tumor using multiple 3D printed soluble filaments, In 2024 IEEE International Symposium of Biomedical Imaging (ISBI), May 2024.

[23] Y. Fan, W. Jiang, Y. Zou, J. Li, J. Chen, & X. Deng, Numerical simulation of pulsatile non-Newtonian flow in the carotid artery bifurcation. Acta Mechanica Sinica, 25(2), 249-255, 2009.

[24] F. M. Davis, A. Obi, & N. Osborne, Carotid body tumors. Extracranial Carotid and Vertebral Artery Disease: Contemporary Management, 253-260, 2018.

[25] K. Kishimoto, T. Ogasawara, & H. Takahira, Influence of tissue stiffness on cavitation cloud formation by high intensity focused ultrasound in agarose gels, Multiphase Science and Technology, 35(4), 2023.